GEOLOGY | THE GEOLOGICAL SOCIETY OF AMERICA®

https://doi.org/10.1130/G50929.1

Manuscript received 13 June 2022
Revised manuscript received 11 November 2022
Manuscript accepted 14 December 2022

Published online 10 February 2023

Pyroxenite melting at subduction zones

Emilie E. Bowman[1] and Mihai N. Ducea[2,1]
[1]Department of Geosciences, University of Arizona, Tucson, Arizona 85721, USA
[2]Faculty of Geology and Geophysics, University of Bucharest, Bucharest 010040, Romania

ABSTRACT

Arc magmatism is thought to be driven by peridotite melting in the mantle wedge. Yet pyroxenites are ubiquitous in the melting region beneath magmatic arcs. Because they typically have lower solidi temperatures and higher melt productivities compared to peridotite, pyroxenites likely play a significant role in magma generation. Here, we use the Zn/Fe ratios of a global database of Pliocene–Holocene primitive arc magmas to show that, as the crustal thickness of the overlying plate increases, so does the proportion of pyroxenite-derived melts relative to peridotite-derived melts. In fact, at arcs with crustal thicknesses >40 km, the majority of magmas are sourced from pyroxenite. Major and trace element geochemistry of pyroxenite melts is consistent with derivation from mafic magmas frozen in the mantle en route to the surface. We hypothesize that, as the thickness of the continental crust increases, the mantle wedge is displaced toward higher pressures and cooler temperatures, thereby lowering the extent of peridotite melting and allowing magmas sourced from the pyroxenite-veined mantle to dominate the arc budget.

INTRODUCTION

At subduction zones, it is widely accepted that magma generation occurs via flux melting of mantle wedge peridotite (Grove et al., 2012). In this model, which has prevailed since the 1970s, H_2O-rich fluids released from the downgoing oceanic slab depress the solidus of the overlying peridotite, allowing partial melting at the temperature and pressure conditions of the mantle wedge. Due to this process, most petrologic and numerical studies evaluating the architecture (Grove et al., 2009), geochemistry (Turner et al., 2016), and ore-forming potential (Rezeau and Jagoutz, 2020) of subduction zones typically assume that primary mafic magmas are predominantly sourced from mantle peridotite, with or without some amount of slab component. The peridotite melting paradigm has further motivated numerous studies investigating the partial melting of (Till et al., 2012) and melt extraction from (Katz et al., 2022) peridotitic lithologies.

The compositional diversity of primitive arc magmas, however, cannot be accomplished by peridotite melting alone, requiring the contribution of nonperidotitic melts to magma generation (Mallik et al., 2021). Due to the prevalence of pyroxenites in the altered oceanic crust (Poli and Schmidt, 2002), mantle wedge (Chapman et al., 2021), and lower crust of the overriding plate (Bowman et al., 2021), primary arc magma production likely involves pyroxenitic sources. For example, it has been well established by thermal (Syracuse et al., 2010) and geochemical (Schmidt and Jagoutz, 2017) studies that the descending, eclogitized oceanic crust can melt in intermediate to hot subduction zones, although the slab contribution is likely subordinate to that of wedge peridotite (Turner et al., 2016). In the mantle wedge of all arcs, pyroxenites may be present as orthopyroxene-rich assemblages formed from melt- and fluid-peridotite reaction (Yaxley and Green, 1998; Grant et al., 2016) and as metasomatic veins crystallized from stalled mafic magmas (Chapman et al., 2021). Additionally, at thick-crusted (>40 km) arcs, magmatic processing in the near-Moho hot zone generates a dense (>3.4 g/cm^3; Bowman et al., 2021) garnet clinopyroxenitic ("arclogitic") residual root that can founder into the mantle and melt as it descends (Ducea et al., 2021).

Based on the abundance of pyroxenites in the melting region of subduction zones as well as the lower solidi temperatures and higher melt productivities of these lithologies compared to peridotite (Lambart et al., 2013), preferential melting of pyroxenite may supply disproportionate volumes of magma to the arc budget, especially at thick-crusted arcs where extents of peridotite melting are suppressed (Turner et al., 2016). However, the role of pyroxenite melting in generating arc magmas has yet to be constrained. In this paper, we evaluate the contribution of peridotite- versus pyroxenite-derived melts to arc magmatism as a function of the crustal thickness of the overriding plate. We use the Zn/Fe ratios, along with other geochemical metrics, of a global database of Pliocene–Holocene primitive arc magmas to show that the proportion of pyroxenite- to peridotite-derived melts increases with increasing crustal thickness, so much so that pyroxenite melts comprise the majority of magmas erupted onto thick crust. These results challenge the validity of the peridotite melting paradigm as it applies to thick-crusted arcs and necessitates a new model for primary magma generation from pyroxenites in these settings.

GLOBAL DATABASE OF PRIMITIVE ARC MAGMAS

Using the GEOROC database (https://georoc.eu/) supplemented by published samples from the Andean arc, we compiled whole-rock compositions of subaerial Pliocene–Holocene primitive magmas (MgO = 7–17 wt%) from 20 frontal arcs around the globe (Fig. S1 in the Supplemental Material[1]). Because primitive magmas rarely erupt in regions of thick crust, we retained rear-arc compositions from the central Andean plateau to ensure a critical number of samples from the thickest (>50 km) arcs. Crustal thicknesses were calculated using the elevation of each sample according to the

[1]Supplemental Material. Data filtering methods, crustal thickness calculations, spatial averaging methods, error calculations, sample locations, Zn/Fe versus Al_2O_3 for subarc peridotites, Zn/Fe-crustal thickness correlation for samples with MgO >10 wt%, Dy/Yb, Ba/Nb, and Th/Nb ratios as a function of crustal thickness, copper contents of peridotite- versus pyroxenite-derived melts, the filtered and spatially averaged global geochemical compilation created and used in this study, and the compilation of experimental melts of silica-deficient pyroxenites. Please visit https://doi.org/10.1130/GEOL.S.21936018 to access the supplemental material, and contact editing@geosociety.org with any questions.

CITATION: Bowman, E.E., and Ducea, M.N., 2023, Pyroxenite melting at subduction zones: Geology, v. 51, p. 383–386, https://doi.org/10.1130/G50929.1

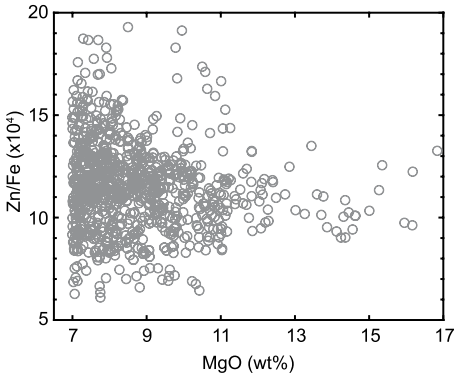

Figure 1. Zn/Fe (×10⁴) of each sample versus MgO content (wt%). The lack of correlation indicates Zn/Fe ratios are not affected by differentiation.

method of Luffi and Ducea (2022). To reduce the effects of sampling bias in our compilation such that each volcanic field is equally represented, we divided the spatial coverage of our data set into prisms 10 km long × 10 km wide × 650 m high and calculated the median geochemical composition and crustal thickness for each volume unit. Geochemical filtering methods, crustal thickness calculations, and the statistical treatment of errors for all parameters are documented in the Supplemental Material.

RESULTS

Zn/Fe ratios have been shown to effectively distinguish peridotite- and pyroxenite-derived magmas (Le Roux et al., 2010, 2011; Lang and Lambart, 2022). Because Zn/Fe undergoes little fractionation between olivine, orthopyroxene, and melt, these ratios are not changed significantly during peridotite partial melting or olivine-only crystallization. However, when garnet and clinopyroxene are major phases, as in pyroxenite, Zn/Fe ratios are highly fractionated during melting. Pyroxenite melts, as a result, can attain Zn/Fe ($\times 10^4$) ratios >12 and as high as 20; in contrast, most peridotite melts have ratios only up to ~12. We note that low-degree (melt fraction [F] < 0.15) melts of the most fertile (Al_2O_3 > 4 wt%), high-Zn/Fe peridotites can achieve Zn/Fe ($\times 10^4$) up to ~13 (Davis et al., 2013) owing to high modes of garnet and clinopyroxene. However, ~85% of subarc peridotites reported in the GEOROC database are not very fertile (Al_2O_3 < 4 wt%; Fig. S2), have Zn/Fe ($\times 10^4$) < 10, and should not produce high (>12)-Zn/Fe melts. The subarc mantle has also been shown to be relatively depleted in composition (Schmidt and Jagoutz, 2017) and is therefore not likely to generate high (>12)-Zn/Fe melts. Because pyroxenites, on the other hand, definitely can generate magmas with Zn/Fe ($\times 10^4$) > 12, we take Zn/Fe ($\times 10^4$) = 12 as the dividing value between peridotite and pyroxenite melts.

Zn/Fe ratios are affected by cotectic differentiation, so we must first verify that the ratios in our database do not derive from multiply saturated magmas. In a plot of Zn/Fe versus MgO content for each sample in the data set (Fig. 1), we find that there is no systematic variation in Zn/Fe ratios with differentiation, lending confidence that our compilation contains only primitive magmas that have undergone olivine-dominated fractionation.

We plot median Zn/Fe ratios, spatially averaged as detailed above, against corresponding median crustal thickness values (Fig. 2A). We also plot these data for samples with >10 wt% MgO (Fig. S3). In both cases, it is clear that Zn/Fe ratios are positively correlated with crustal thickness. Specifically, Zn/Fe ratios steadily rise as crustal thickness increases from <30 to 40 km, although the majority of median samples in this thickness range have Zn/Fe ($\times 10^4$) < 12 and are likely sourced primarily from peridotite. Once crustal thickness exceeds ~40 km, however, the majority of the database has Zn/Fe ($\times 10^4$) > 12, indicating pyroxenite-dominant melting in thick-crusted regions. Median Dy/Yb ratios of primitive magmas also seem to increase with crustal thickness (Fig. S4A), further supporting garnet-present melting beneath thick arcs (Davidson et al., 2007).

To evaluate the legitimacy of the observed Zn/Fe–crustal thickness correlation, the spatially averaged Zn/Fe database was further binned into 5 km crustal thickness intervals from <30 to >60 km (Fig. 2B). Here, an increase in Zn/Fe ratios with increasing crustal thickness is remarkably apparent. Weighted linear regression (Thirumalai et al., 2011) through these data yields a trendline with an R^2 value of 0.97, confirming the reliability of this correlation. We note that for crustal thicknesses >50 km, comparatively few data exist (n < 15 for each crustal thickness bin), and 64% of this median data set is from the central Andes. Removal of this crustal thickness range produces a very similar array (Fig. 2B), indicating that magmas emplaced in the frontal to rear arc of the central Andes conform to the global pattern of Zn/Fe variability. Finally, we recognize that high-Zn/Fe melts can derive from mantle peridotites enriched in Zn via fluid-induced metasomatism (Le Roux et al., 2010). However, complete overlap in the Ba/Nb ratios of high (>12)- and low (<12)-Zn/Fe melts (Fig. S4B; Elliot, 2003), as well as the global lack in correlation between crustal thickness and regions of metasomatized mantle (Qin et al., 2022), invalidate this possibility.

To further elucidate the source of high-Zn/Fe melts in our compilation, we plot these samples on the pseudo-ternary diagram forsterite–calcium Tschermak's pyroxene (CaTs)–quartz projected from diopside (Fig. 3). When garnet and pyroxene are primary residual phases, a thermal barrier marked by the enstatite-CaTs join segregates the compositions of melts derived from

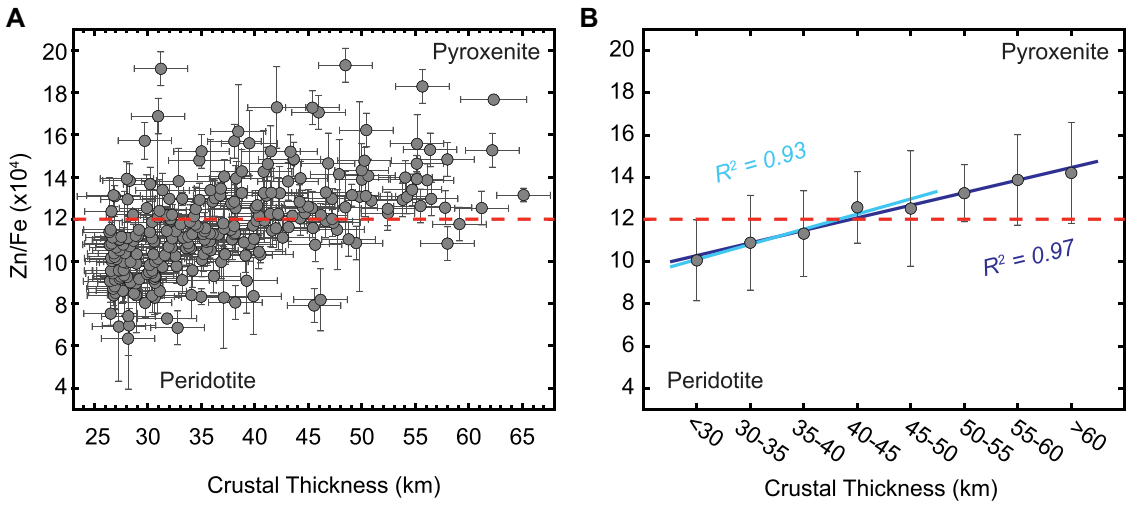

Figure 2. (A) Correlation of median Zn/Fe ratios with crustal thickness. Errors on Zn/Fe (×10⁴) are 1σ standard deviations. Errors on crustal thickness are root mean square errors. (B) Median Zn/Fe ratios binned into 5 km crustal thickness intervals. Errors are root mean square errors. Weighted regression (dark blue line) through these data yields a trendline with R^2 = 0.97. Weighted regression (light blue, R^2 = 0.93) was calculated for crustal thicknesses <50 km to remove the effect of few data at thick-crusted arcs as well as the influence of the Andean arc on the Zn/Fe–crustal thickness correlation. For both panels, the red dashed line delineates the fields of peridotite (Zn/Fe [×10⁴] < 12) and pyroxenite (Zn/Fe [×10⁴] > 12) melts.

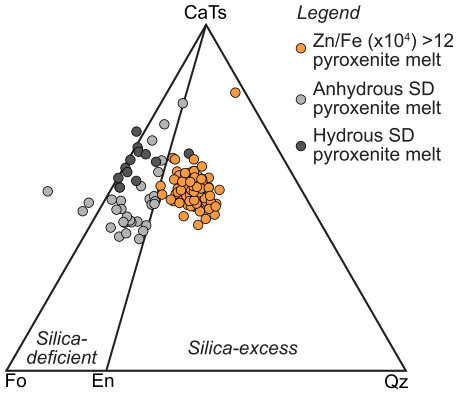

Figure 3. Projection from diopside (Di) on forsterite (Fo)–calcium Tschermak's pyroxene (CaTs)–quartz (Qz) pseudo-ternary diagram (O'Hara, 1972) of spatially averaged samples with median Zn/Fe (×10⁴) > 12. The enstatite (En)–CaTs join separates silica-deficient and silica-excess melts. Experimental melts of silica-deficient (SD) pyroxenites are also plotted (see the Supplemental Material [see footnote 1] for compilation and references).

silica-excess and silica-deficient pyroxenites (Kogiso et al., 2004). Because the high-Zn/Fe samples plot firmly on the silica-excess side of the ternary diagram, such melts are likely sourced from silica-excess pyroxenites. This origin for the high-Zn/Fe magmas is consistent with their SiO_2 and alkali contents (Lambart et al., 2013), which are distinctly elevated compared to those of the low-Zn/Fe samples (Fig. 4).

NATURE OF THE PYROXENITE SOURCE

Based on Zn/Fe ratios and major element geochemistry, we argue that the proportion of arc magmas derived from pyroxenite versus peridotite increases with crustal thickness. In particular, at arcs with crustal thicknesses >40 km, pyroxenites rather than peridotites dominate the source of primary magmas. Is it possible to constrain the nature of the pyroxenitic source that is melting beneath thick-crusted arcs? In these regions, pyroxenite melts may derive from the eclogitized oceanic crust, products of melt- and fluid-rock reaction, lower crustal and/or foundering arclogite, or metasomatic mantle veins representing solidified mafic intrusions. Because magmas at thick-crusted arcs have isotopic compositions inconsistent with a mid-ocean ridge basalt (MORB)–like source (Ducea and Barton, 2007), melting of the oceanic crust is probably not the predominant mechanism of magmagenesis. Th/Nb ratios, a particularly diagnostic tracer of slab melt (Fig. S4C; Turner and Langmuir, 2022), are also independent of source lithology, further precluding a primary role of the slab in generating high-Zn/Fe magmas. It is also unlikely that pyroxenites formed from melt- and fluid-rock reaction contribute significantly to magmatism at thick-crusted arcs, as these assemblages are typically rich in olivine (Kelemen et al., 1995) or orthopyroxene (Yaxley and Green, 1998; Grant et al., 2016), depending on the reactants, and should produce magmas with low Zn/Fe ratios. Furthermore, residual arclogites may melt via heating and/or amphibole dehydration to form silica-deficient melts (Fig. 3; Ducea et al., 2021). High-Zn/Fe melts in our data set, however, lie on the silica-excess side of the garnet-pyroxene thermal barrier and are on average too silica-rich to be sourced from arclogite.

We favor a model in which the majority of magmas erupted at thick-crusted (>40 km) arcs originate from veins of peridotite-derived mafic melts frozen during ascent into the cooler asthenospheric wedge and/or mantle lithosphere. Such veins will be silica-excess pyroxenites composed of clinopyroxene + garnet ± orthopyroxene ± amphibole ± plagioclase (Rapp and Watson, 1995). If these pyroxenitic veins are later relocated to the melting region of the mantle wedge due to, e.g., mantle flow or landward arc migration (Chapman et al., 2021), they will partially melt via reheating or volatile fluxing. Partial melts sourced from these lithologies will be comparatively silica- and alkali-rich (Lambart et al., 2013) with high Zn/Fe ratios, consistent with our suite of pyroxenite-derived samples (Fig. 4).

As the crustal thickness of volcanic arcs increases, the mantle wedge is shifted toward higher pressures and colder temperatures (Turner et al., 2016), resulting in lower degrees of melting of the peridotitic mantle. Pyroxenites, on the other hand, have solidi temperatures ~50–150 °C lower than peridotites (Hirschmann and Stolper, 1996). Such low melting temperatures and higher melt productivities ($F = 0.15$–0.3; Chapman et al., 2021) compared to peridotite ($F = 0.05$–0.15 at similar conditions; Grove et al., 2012), along with the diffusive influx of heat from ambient subsolidus peridotites to melting pyroxenitic veins (Hirschmann and Stolper, 1996), allow pyroxenites to produce significant amounts of melt at the temperatures of the mantle wedge, even if present in insignificant volumes (Lambart et al., 2013). Based on the observed correlation between Zn/Fe ratios and crustal thickness as well as the geochemistry of high-Zn/Fe melts, we propose that the pressure-temperature conditions of the subarc mantle become less favorable for peridotite melting once the crust reaches ~40 km in thickness. At this point, pyroxenitic veins in the asthenospheric wedge and/or mantle lithosphere contribute the bulk of the magmatic budget. This is especially likely since frozen mantle-derived melts have been estimated to comprise up to 30% of the subarc lithospheric mantle (Chin et al., 2014). In fact, in their model of Cordilleran arcs (crustal thickness >45 km), Chapman et al. (2021) attribute periods of high-flux magmatism to enhanced melting of lithosphere metasomatized by melt-fertile mafic intrusions.

We emphasize that our interpretations do not consider the effects of amphibole on Zn/Fe fractionation because experimental amphibole-melt Zn and Fe partition coefficients for basaltic compositions are lacking. Nevertheless, pyroxenites usually contain only minor abundances of amphibole, which may even be completely absent at pressures >2.5 GPa (Wyllie and Wolf, 1993). Amphibole, if present, is also exhausted early during melting. Therefore, the presence of amphibole in pyroxenitic assemblages is unlikely to shift the Zn/Fe ratios of the derivative magma into the realm of peridotite-sourced values.

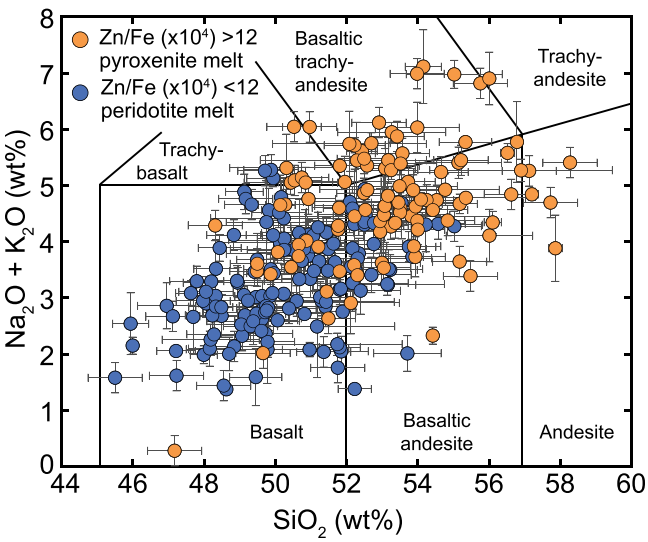

Figure 4. Total alkali-silica diagram of the spatially averaged data set colored according to median Zn/Fe (×10⁴). Compared to low (<12)-Zn/Fe melts, high (>12)-Zn/Fe magmas are more silica- and alkali-rich. Errors are 1σ standard deviations. Samples ($n = 4$) with errors of >3 and >1 wt% on SiO_2 and $Na_2O + K_2O$, respectively, are not plotted.

IMPLICATIONS

In light of our findings, most models of subduction zones applicable to thick-crusted arcs must be updated to consider pyroxenites as the dominant source of primary arc magmas in these settings. Because pyroxenites have lower

solidi temperatures compared to peridotites, we expect substantial modifications to numerical and conceptual models that have traditionally assumed a peridotite solidus (e.g., Grove et al., 2009). In addition, Cu contents of pyroxenite-derived melts are systematically lower than those sourced from peridotite (Fig. S5). Perhaps pyroxenites are inherently Cu-poor, or the presence of Cu-sulfides in these lithologies cause Cu to act compatibly during melting. Either way, because porphyry copper deposits preferentially form in regions of thick crust (Chiaradia, 2014), it is imperative that we constrain the role, if any, of pyroxenite melting in controlling the ore-forming potential of arc magmas.

ACKNOWLEDGMENTS

We acknowledge support from a U.S. National Science Foundation Frontier Research in Earth Sciences (NSF-FRES) grant (EAR2020935) and Romanian Ministry of Research, Innovation and Digitalization (MCID) project C1.2.PFE-CDI.2021-587 (contract 41PFE/30.12.2021). We thank the University of Bucharest for providing funds to publish under Gold Open Access. Discussions with Kaustubh Thirumalai and feedback from two anonymous reviewers greatly improved the manuscript.

REFERENCES CITED

Bowman, E.E., Ducea, M.N., and Triantafyllou, A., 2021, Arclogites in the subarc lower crust: Effects of crystallization, partial melting, and retained melt on the foundering ability of residual roots: Journal of Petrology, v. 62, egab094, https://doi.org/10.1093/petrology/egab094.

Chapman, J.B., Shields, J.E., Ducea, M.N., Paterson, S.R., Attia, S., and Ardill, K.E., 2021, The causes of continental arc flare ups and drivers of episodic magmatic activity in Cordilleran orogenic systems: Lithos, v. 398–399, 106307, https://doi.org/10.1016/j.lithos.2021.106307.

Chiaradia, M., 2014, Copper enrichment in arc magmas controlled by overriding plate thickness: Nature Geoscience, v. 7, p. 43–46, https://doi.org/10.1038/ngeo2028.

Chin, E.J., Lee, C.-T.A., and Barnes, J.D., 2014, Thickening, refertilization, and the deep lithosphere filter in continental arcs: Constraints from major and trace elements and oxygen isotopes: Earth and Planetary Science Letters, v. 397, p. 184–200, https://doi.org/10.1016/j.epsl.2014.04.022.

Davidson, J., Turner, S., Handley, H., Macpherson, C., and Dosseto, A., 2007, Amphibole "sponge" in arc crust?: Geology, v. 35, p. 787–790, https://doi.org/10.1130/G23637A.1.

Davis, F.A., Humayun, M., Hirschmann, M.M., and Cooper, R.S., 2013, Experimentally determined mineral/melt partitioning of first-row transition elements (FRTE) during partial melting of peridotite at 3 GPa: Geochimica et Cosmochimica Acta, v. 104, p. 232–260, https://doi.org/10.1016/j.gca.2012.11.009.

Ducea, M.N., and Barton, M.D., 2007, Igniting flare-up events in Cordilleran arcs: Geology, v. 35, p. 1047–1050, https://doi.org/10.1130/G23898A.1.

Ducea, M.N., Chapman, A.D., Bowman, E., and Balica, C., 2021, Arclogites and their role in continental evolution; Part 2: Relationship to batholiths and volcanoes, density and foundering, remelting and long-term storage in the mantle: Earth-Science Reviews, v. 214, 103476, https://doi.org/10.1016/j.earscirev.2020.103476.

Elliott, T.R., 2003, Tracers of the slab, *in* Eiler, J., ed., Inside the Subduction Factory: American Geophysical Union Geophysical Monograph 138, p. 23–45, https://doi.org/10.1029/138GM03.

Grant, T.B., Harlov, D.E., and Rhede, D., 2016, Experimental formation of pyroxenite veins by reactions between olivine and Si, Al, Ca, Na, and Cl-rich fluids at 800 °C and 800 MPa: Implications for fluid metasomatism in the mantle wedge: American Mineralogist, v. 101, p. 808–818, https://doi.org/10.2138/am-2016-5441.

Grove, T.L., Till, C.B., Lev, E., Chatterjee, N., and Médard, E., 2009, Kinematic variables and water transport control the formation and location of arc volcanoes: Nature, v. 459, p. 694–697, https://doi.org/10.1038/nature08044.

Grove, T.L., Till, C.B., and Krawczynski, M.J., 2012, The role of H_2O in subduction zone magmatism: Annual Review of Earth and Planetary Sciences, v. 40, p. 413–439, https://doi.org/10.1146/annurev-earth-042711-105310.

Hirschmann, M.M., and Stolper, E.M., 1996, A possible role for garnet pyroxenite in the origin of the "garnet signature" in MORB: Contributions to Mineralogy and Petrology, v. 124, p. 185–208, https://doi.org/10.1007/s004100050184.

Katz, R.F., Rees Jones, D.W., Rudge, J.F., and Keller, T., 2022, Physics of melt extraction from the mantle: Speed and style: Annual Review of Earth and Planetary Sciences, v. 50, p. 507–540, https://doi.org/10.1146/annurev-earth-032320-083704.

Kelemen, P.B., Shimizu, N., and Salters, V.J.M., 1995, Extraction of mid-ocean-ridge basalt from the upwelling mantle by focused flow of melt in dunite channels: Nature, v. 375, p. 747–753, https://doi.org/10.1038/375747a0.

Kogiso, T., Hirschmann, M.M., and Pertermann, M., 2004, High-pressure partial melting of mafic lithologies in the mantle: Journal of Petrology, v. 45, p. 2407–2422, https://doi.org/10.1093/petrology/egh057.

Lambart, S., Laporte, D., and Schiano, P., 2013, Markers of the pyroxenite contribution in the major-element compositions of oceanic basalts: Review of the experimental constraints: Lithos, v. 160–161, p. 14–36, https://doi.org/10.1016/j.lithos.2012.11.018.

Lang, O.I., and Lambart, S., 2022, First-row transition elements in pyroxenites and peridotites: A promising tool for constraining mantle source mineralogy: Chemical Geology, v. 612, p. 121137, https://doi.org/10.1016/j.chemgeo.2022.121137.

Le Roux, V., Lee, C.-T.A., and Turner, S.J., 2010, Zn/Fe systematics in mafic and ultramafic systems: Implications for detecting major element heterogeneities in the Earth's mantle: Geochimica et Cosmochimica Acta, v. 74, p. 2779–2796, https://doi.org/10.1016/j.gca.2010.02.004.

Le Roux, V., Dasgupta, R., and Lee, C.-T.A., 2011, Mineralogical heterogeneities in the Earth's mantle: Constraints from Mn, Co, Ni and Zn partitioning during partial melting: Earth and Planetary Science Letters, v. 307, p. 395–408, https://doi.org/10.1016/j.epsl.2011.05.014.

Luffi, P., and Ducea, M.N., 2022, Chemical mohometry: Assessing crustal thickness of ancient orogens using geochemical and isotopic data: Reviews of Geophysics, v. 60, e2021RG000753, https://doi.org/10.1029/2021RG000753.

Mallik, A., Lambart, S., and Chin, E.J., 2021, Tracking the evolution of magmas from heterogeneous mantle sources to eruption, *in* Marquardt, H., et al., eds., Mantle Convection and Surface Expressions: American Geophysical Union Geophysical Monograph 263, p. 151–177, https://doi.org/10.1002/9781119528609.ch6.

O'Hara, M.J., 1972, Data reduction and projection schemes for complex compositions, *in* Biggar, G.M., ed., Progress in Experimental Petrology: Manchester, Edinburgh, Natural Environment Research Council, p. 103–126.

Poli, S., and Schmidt, M.W., 2002, Petrology of subducted slabs: Annual Review of Earth and Planetary Sciences, v. 30, p. 207–235, https://doi.org/10.1146/annurev.earth.30.091201.140550.

Qin, B., Huang, F., Huang, S.C., Python, A., Chen, Y.F., and ZhangZhou, J., 2022, Machine learning investigation of clinopyroxene compositions to evaluate and predict mantle metasomatism worldwide: Journal of Geophysical Research: Solid Earth, v. 127, e2021JB023614, https://doi.org/10.1029/2021JB023614.

Rapp, R.P., and Watson, E.B., 1995, Dehydration melting of metabasalt at 8–32 kbar: Implications for continental growth and crust-mantle recycling: Journal of Petrology, v. 36, p. 891–931, https://doi.org/10.1093/petrology/36.4.891.

Rezeau, H., and Jagoutz, O., 2020, The importance of H_2O in arc magmas for the formation of porphyry Cu deposits: Ore Geology Reviews, v. 126, 103744, https://doi.org/10.1016/j.oregeorev.2020.103744.

Schmidt, M.W., and Jagoutz, O., 2017, The global systematics of primitive arc melts: Geochemistry, Geophysics, Geosystems, v. 18, p. 2817–2854, https://doi.org/10.1002/2016GC006699.

Syracuse, E.M., van Keken, P.E., and Abers, G.A., 2010, The global range of subduction zone thermal models: Physics of the Earth and Planetary Interiors, v. 183, p. 73–90, https://doi.org/10.1016/j.pepi.2010.02.004.

Thirumalai, K., Singh, A., and Ramesh, R., 2011, A MATLAB™ code to perform weighted linear regression with (correlated or uncorrelated) errors in bivariate data: Journal of the Geological Society of India, v. 77, p. 377–380, https://doi.org/10.1007/s12594-011-0044-1.

Till, C.B., Grove, T.L., and Withers, A.C., 2012, The beginnings of hydrous mantle wedge melting: Contributions to Mineralogy and Petrology, v. 163, p. 669–688, https://doi.org/10.1007/s00410-011-0692-6.

Turner, S.J., and Langmuir, C.H., 2022, An evaluation of five models of arc volcanism: Journal of Petrology, v. 63, egac010, https://doi.org/10.1093/petrology/egac010.

Turner, S.J., Langmuir, C.H., Katz, R.F., Dungan, M.A., and Escrig, S., 2016, Parental arc magma compositions dominantly controlled by mantle-wedge thermal structure: Nature Geoscience, v. 9, p. 772–776, https://doi.org/10.1038/ngeo2788.

Wyllie, P.J., and Wolf, M.B., 1993, Amphibolite dehydration-melting: Sorting out the solidus, *in* Prichard, H.M., et al., eds., Magmatic Processes and Plate Tectonics: Geological Society, London, Special Publication 76, p. 405–416, https://doi.org/10.1144/GSL.SP.1993.076.01.20.

Yaxley, G., and Green, D., 1998, Reactions between eclogite and peridotite: Mantle refertilisation by subduction of oceanic crust: Schweizerische Mineralogische und Petrographische Mitteilungen, v. 78, p. 243–255.

Printed in USA